Histomorphological Changes in Experimental Autoimmune Uveitis of Varying Severity

Kuryltsiv Nadiia

DNP "Danylo Halytsky Lviv National Medical University", Lviv, Ukraine

MD Nadiia Kuryltsiv, PhD

Submitted to the editorial board: December 11, 2025
Accepted for publication: April 24, 2026
Available on-line: June 1, 2026

The authors of the study declare that no conflict of interest exists in the compilation, theme and subsequent publication of this professional communication, and that it is not supported by any pharmaceutical company. The study has not been submitted to another journal and is not printed elsewhere, with the exception of congress summaries and recommended procedures.

Correspondence address:
MD Nadiia Kuryltsiv, PhD
69 Pekarska str
Lviv
Ukraine 79010
E-mail: kuryltsivnb@gmail.com

SUMMARY

Aim: to evaluate the histomorphology of the eyes of rabbits with experimental autoimmune uveitis (EAU) of varying severity.
Materials and Methods: The study was conducted on 30 Chinchilla rabbits with EAU, which were divided into two groups according to the severity of the disease. Histomorphological examination of the rabbit eyes was performed.
Results: In general, the inflammatory process can be characterized as a humoral-type hypersensitivity reaction. An inflammatory process was observed, predominantly affecting the inner ocular layers – mainly the choroid and retina. Inflammatory changes in the iris were sporadic, minimal, and primarily consisted of a few scattered lymphocyte-like cells. In the ciliary body, inflammation predominantly involved the ciliary processes. Damage to the retinal pigment epithelium was predominantly observed in the optical part. The involvement of the choroidal vasculature was evident, accompanied by stromal exudation. Retinal alterations predominantly involved the inner layers.
The bipolar and ganglion cell layers were essentially destroyed, while the photoreceptor layer was largely preserved. Destruction of the retinal pigment epithelium was associated with damage to Bruch's membrane.
Conclusion: Overall, histomorphological alterations in EAU showed a time-dependent progression, peaking between Days 3 and 10, particularly in moderate and severe cases. Although inflammatory activity decreased from Day 14 onward, complete morphological recovery was not observed. Persistent intergroup differences indicate sustained, partially irreversible ocular tissue damage associated with disease severity.
Key words: histomorphology, experimental model, autoimmune uveitis, tissue damage

Čes. a slov. Oftal., 82, 2026, No. x, p.

INTRODUCTION

In the comprehensive investigation of autoimmune uveitis, alongside the assessment of clinical progression and immunological alterations, a detailed evaluation of histomorphological changes – specifically the characterization of target tissue involvement – represents an essential component for understanding the disease mechanisms. Of particular interest is the understanding of tissue and ocular structural damage in autoimmune uveitis of varying degrees of severity. Histomorphological investigations provide essential insights into the complex mechanisms of uveitis, by elucidating the interactions between various ocular cells and tissues during the inflammatory process. By monitoring histomorphological alterations, investigators can evaluate the therapeutic efficacy of various interventions in attenuating inflammation and limiting tissue injury [1,2]. According to the literature, uveitis predominantly affects young individuals and leads to significant visual impairment in approximately 35% of cases [3–5].

Due to the importance of obtaining morphological samples in humans, models of endogenous uveitis have been developed. This has made it possible to study the pathogenetic mechanisms of this disease [6–8].

The rabbit model of uveitis is characterized by several advantages over other experimental models. The rabbit eye is comparable in size to the human eye, which facilitates anatomical orientation of ocular structures and allows superior visualization for histomorphological analysis [9]. Secondly, the layers of the iris, ciliary body, and choroid are more distinctly differentiated in the rabbit

eye, enabling more accurate assessment of inflammatory infiltration, edema, and vasculitis [9]. In experimental studies of uveitis, the rabbit model is therefore considered optimal, particularly in the absence of genetic or molecular investigations, which are more appropriately conducted using murine models [10,11].

Objectives: to evaluate the histomorphology of the eyes of rabbits with experimental autoimmune uveitis (EAU) of varying severity.

MATERIALS AND METHODS

The study was conducted on 30 Chinchilla rabbits, aged 90–120 days and weighing 2.5–3.0 kg, which were kept under standard vivarium conditions. All rabbits underwent a two-week quarantine period prior to the experiments. In this study, a previously established model of autoimmune uveitis was modified [12,13]. EAU was induced, following the protocol described by Kuryltsiv and colleagues [14]. All rabbits were pre-sensitized by 1.0 ml of normal horse serum (Biolyk (UA) intravenous injection daily for 5 days. Ten days after the final injection, rabbits in Group I (n = 15) received an intravitreal injection of 0.1 ml of undiluted normal sterile horse serum in both eyes. An intravitreal injection of 0.1 ml of normal sterile horse serum, diluted with saline at a 1:2 ratio, was administered to rabbits in Group II (n = 15) in both eyes. As a result, uveitis of varying severity was observed: Group I included rabbits with moderate to severe EAU, while Group II comprised rabbits with mild EAU.

On the designated experimental days of sacrifice (days 3, 7, 10, 14, and 21), histomorphological examination of the rabbit eyes was performed on all 60 paired eyes enucleated from 30 rabbits (in Group 1 – 30 eyes, in Group II – 30 eyes). The specimens were fixed in 10% neutral formalin and processed according to standard procedures for paraffin embedding. Two blocks were prepared from each eye, from which up to 10 serial sections were obtained and stained with hematoxylin and eosin. Microscopic analysis of the sections was carried out, using a Jenamed-2 light microscope at both low and high magnifications, employing 10×, 40×, and 60× objectives. Photo-documentation was performed, using a DCM-1.30mp digital video camera. Selection and editing of microphotographs were conducted, including removal of minor technical artifacts, using the Microsoft Paint raster graphics editor.

All animal experiments were performed in compliance with the Law of Ukraine on Protection of Animals from Cruel Treatment No. 3447-IV dated 21.02.2006, European Convention for the Protection of Vertebrate Animals Used for Experimental and Other Scientific Purposes from the European Treaty Series (Strasbourg, 1986), and the WMA Declaration of Helsinki: "Guidelines for the use of experimental animals in experimental research" from 1964–2000, as well as Council Directive 2010/63/EU.

RESULTS

In the majority of eyes, an inflammatory process was observed, predominantly affecting the inner ocular layers – mainly the choroid and retina – including both the optic part of the retina and the ora serrata. In the limbal vessels of the cornea, mild perivascular infiltration was noted in some cases, without an exudative component or involvement of the corneal stroma or drainage structures. Inflammatory changes in the iris were sporadic, minimal, and primarily consisted of a few scattered lymphocyte-like cells. In the ciliary body, inflammation predominantly involved the ciliary processes.

Overall, the inflammatory process can be characterized as a humoral-type hypersensitivity reaction, predominated by lymphocyte-histiocyte-type cells, without involvement of segmented neutrophils. Plasma cells (with eccentrically placed nuclei and a patch of weakly eosinophilic cytoplasm) and tissue basophils (mast cells-with central nuclei and a rim of weakly basophilic cytoplasm) constituted a significant component of the inflammatory infiltrate. In humans, these cells are typically recruited during immunological responses involving IgE antibodies. Mast cells are also characteristic of immunological reactions in animals.

Based on the nature of the cellular response and the accompanying tissue changes, it can be inferred that this hypersensitivity reaction began to develop within the first day following exposure to the corresponding antigen, proceeding as a cytotoxic-type reaction. The probable sites for the binding of cytotoxic antibodies were Bruch's membrane and adjacent membranous structures of the ciliary body processes and vessel walls.

Damage to the pigment epithelium was predominantly observed in the optical part of the retina. The iris was minimally involved in the pathological process while, in the ciliary processes and the ora serrata, the lesions were primarily localized to the zonular fibers and preretinal area. This suggests an association with impaired barrier function of the collagen-elastic membranes, namely Bruch's membrane and the basal membranes of the ciliary process epithelium and the non-optical portion of the retina.

The involvement of the choroidal vasculature was also evident, as demonstrated morphologically by marked vascular dilation, frequently accompanied by stromal exudation within the uveal tract and, in some cases, partial detachment. A similar response was less pronounced in the vessels of the ciliary processes and was only minimally observed in the iris vasculature.

Changes within the retina were markedly pronounced in some cases and exceeded the severity of the uveal response. These alterations predominantly involved the inner retinal layers, indicating that the inflammatory process in the retina was mediated primarily through vascular involvement. This is further supported by the substantial inflammatory activity observed in the preretinal layer and vitreous body, where intense inflammatory infiltration

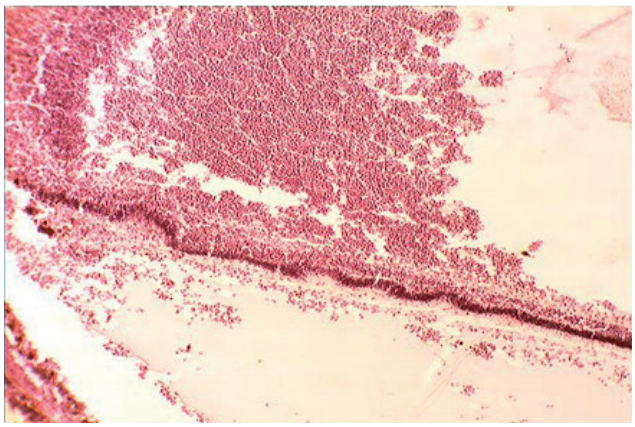

Figure 1. The retina is detached by exudate. All retinal layers, except for the outer nuclear layer, are displaced by a massive inflammatory infiltrate that extends into the vitreous body. H&E staining. Magnification 100×

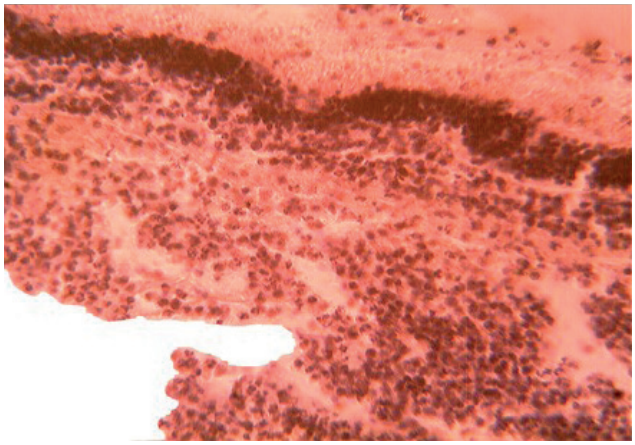

Figure 2. Higher-magnification view of the previous figure. The inflammatory infiltrate consists of lymphocytes, plasma cells, and mast cells. In the upper portion of the image, a layer of photoreceptor cells is visible. H&E staining. Magnification 400×

Figure 3. Diffuse infiltration of the choroid and retina by lymphocytic cells with retinal detachment. Markedly dilated choroidal vessels are visible. The retina is detached together with the disintegrated retinal pigment epithelial cell layer. H&E staining. Magnification 100×

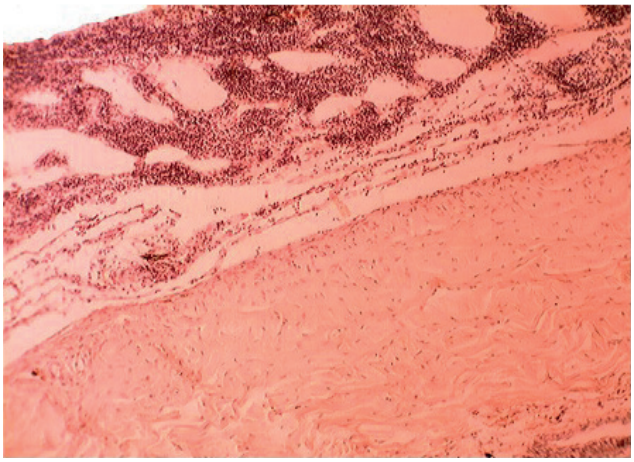

Figure 4. Infiltrate in the posterior choroid. Vascular congestion, edema, and choroidal detachment

was occasionally present. The bipolar and ganglion cell layers were essentially destroyed, while the photoreceptor layer was largely preserved, confirming that the pathological process involved the retinal vasculature, which is confined to the inner retinal layers.

Destruction of the retinal pigment epithelium was associated with damage to the tapetoretinal zone (Bruch's membrane). Consequently, no destructive retinal pigment epithelium changes were observed in the regions of the iris or the ciliary processes. The exudative retinal detachment was likewise linked to alterations within the tapetoretinal zone – primarily involving the retinal pigment epithelium layer – which in many cases separated (desquamated) together with the neurosensory retina.

In the two experimental groups in which autoimmune uveitis of varying severity was induced, the morphological findings showed certain distinctions. In rabbits of Group I, in which undiluted normal sterile horse serum was injected intravitreally, the signs of anterior and posterior uveitis were more pronounced, with a greater number of intraocular structures involved in the inflammatory process.

Specifically, in a subset of Group I specimens, the histological appearance of the eye was as follows (Figure 1): a small number of lymphocytes adjacent to the scleral vessels at the limbus. Clusters of lymphocytes were present in the superficial layers of the pars plana and within the ciliary processes, with diffuse extension toward the zonular fibers. At the choroid, from the ora serrata to the optic nerve head, inflammatory infiltration was noted, predominantly localized along the interface with the retinal pigment epithelium (Figure 2). The retinal pigment epithelium layer demonstrated areas of disruption. The inflammatory infiltrate extended diffusely into the retina, leading to obliteration of the neural layers, with only photoreceptors remaining visible in some regions.

As demonstrated in Figures 3 and 4, in a subset of samples, intense inflammatory infiltration was observed in the limbal region. The iris contained only sparse, scattered inflammatory cells. The zonular fibers exhibited

dense infiltration with preretinal foci; in some areas, the retina was detached by exudate containing cellular elements. Over most of its extent, the retinal architecture was disrupted, with preservation limited to the photoreceptor layer, while the retinal pigment epithelium was disintegrated. Marked diffuse infiltration was present in the choroid. Small clusters of inflammatory cells were also noted within the optic nerve sheaths.

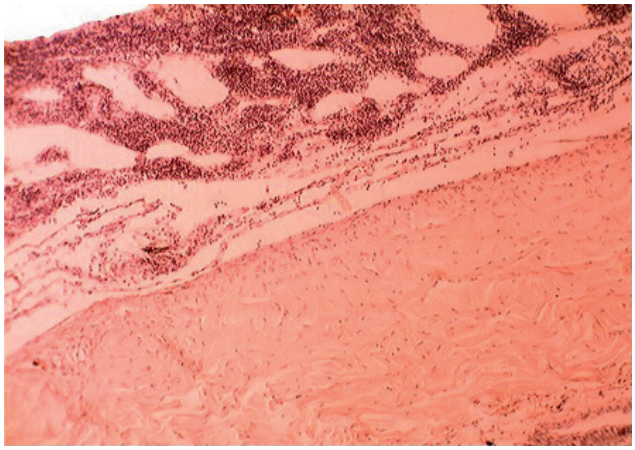

Figure 5. Moderate inflammatory infiltration was observed within the zonular fibers (1) and the ciliary processes (2). H&E staining. Magnification 200×

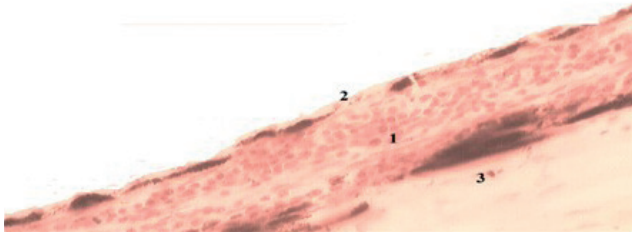

Figure 6. Moderate inflammatory infiltration (1) was present within the choroid. The retinal pigment epithelium exhibited focal areas of desquamation (2). In the sclera (3), focal accumulations of melanocytes were observed. H&E staining. Magnification 100×

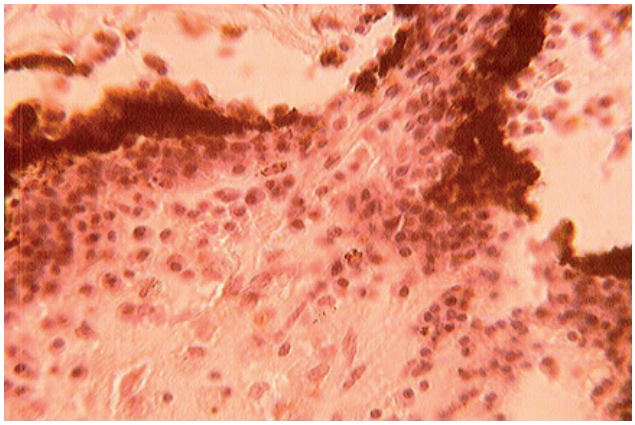

Figure 7. Infiltration in the region of the zonular fibers. The infiltrate is predominantly composed of plasma cell–type elements and mast cells. H&E staining. Magnification 600×

At the same time, a portion of the specimens demonstrated the following changes: in the conjunctiva at the limbal region, a few small scattered lymphocytes were present. The iris contained dispersed lymphocytic infiltrates, with a focal accumulation near the iris root, extending toward the drainage angle. Inflammatory infiltration was detected within the ciliary processes and the zonular fibers (Figure 5). In the choroid, inflammatory infiltrates were noted near the ora serrata and around the optic nerve head, while the remainder of the choroid appeared normal (Figure 6). In the optic nerve head and the adjacent retina, scattered lymphocytes were identified; the retina was unremarkable throughout most of its extent.

In the analysis of specimens from Group II, in a small number of histological specimens, the inflammatory changes in the anterior segment were mild (Figures 7, 8). The ciliary processes contained occasional inflammatory cells, with a moderate infiltrate in the zonular fibers. A small cluster of inflammatory cells was observed in the anterior chamber angle. The choroid and retina were normal throughout their entire extent.

The histomorphological profile indicated a more pronounced severity of uveitis, as evidenced by the following changes: as shown in Figure 9, small foci of lymphocytic

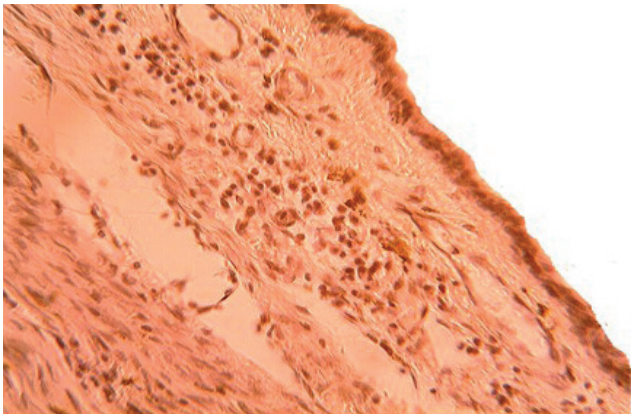

Figure 8. Mild limbal infiltration characterized by scattered small lymphocytic cells. H&E staining. Magnification 400×

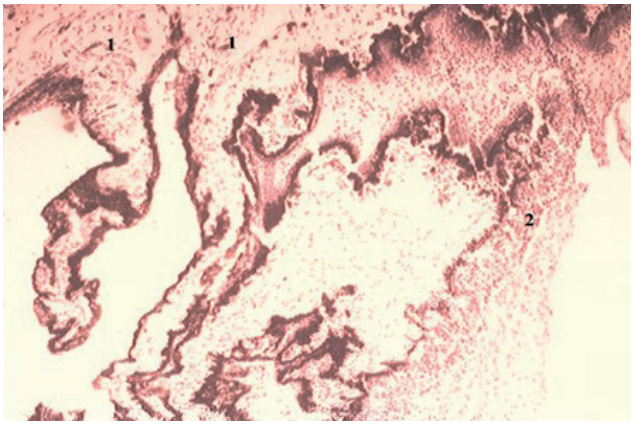

Figure 9. Lymphocytic infiltrates were present in the ciliary body (1) near the ora serrata, extending to the zonular fibers (2). H&E staining. Magnification 100×

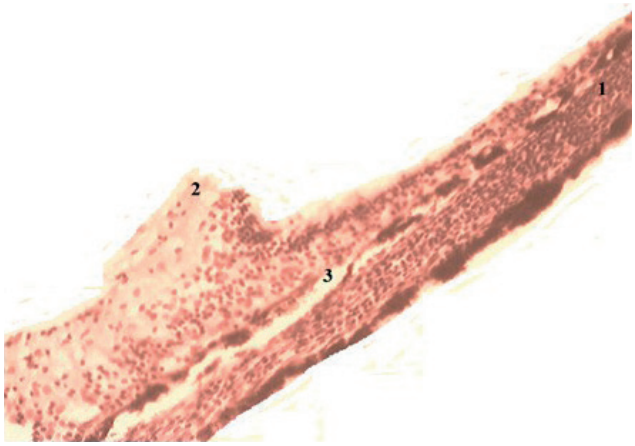

Figure 10. In the choroid near the ora serrata, lymphocytic infiltrates (1) were observed, extending into the subretinal space (2), accompanied by desquamation of the retinal pigment epithelium (3). H&E staining. Magnification 200×

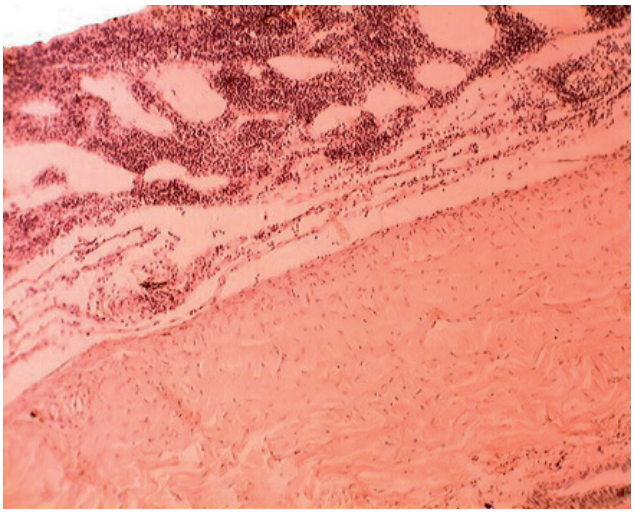

Figure 11. Lymphocytic aggregates in the preretinal region and withn the optic nerve head. H&E staining. Magnification 100×

Table 2. Histomorphological change scores in Group I and Group II

Experimental day	Me (Q_I – Q_{III})		P value
	Group I	Group II	
Day 3 (n1 = 30, n2 = 30)	13 (11.25–14)	6 (4–7)	**< 0.001**
Day 7 (n1 = 26, n2 = 26)	14 (13–16)	8 (8–9)	**< 0.001**
Day 10 (n1= 22, n2 = 22)	16 (15–17)	8 (7.25–9.75)	**< 0.001**
Day 14 (n1 = 18, n2 = 18)	14 (13–15)	7 (5.25–7)	**< 0.001**
Day 21 (n1 = 14, n2 = 14)	11.50 (10–12)	4 (3–4)	**< 0.001**
Day 30 (n1 = 10, n2 = 10)	7 (6–8)	3 (2.25–3.75)	**< 0.001**

Comparisons were performed using the Mann–Whitney U test, p<0.05 – statistically significant difference between Group I and Group II, ME – median, n1 – numbers of rabbits in group I, n2 – numbers of rabbits in group II, Q_I – Q_{III} – interquartile range

infiltration in the limbal region; lymphocytic infiltrates in the ciliary body near the ora serrata, extending toward the zonular fibers; a mild infiltrate within the drainage angle. In the choroid, isolated foci of infiltration were observed as minor focal thickenings (up to 300 μm) (Figure 10). In the retina, scattered clusters of lymphocytes were present preretinally and within the optic nerve head (Figure 11).

We developed a scoring system to assess the structural damage of the ocular globe in uveitis (Table 1). This scoring system enabled quantitative statistical comparison of the severity of ocular involvement between the two study groups at each predefined experimental time point.

Based on these data, a statistical analysis was performed. A comparative assessment of the mean histomorphological change scores at the experimental time points was obtained and is presented in Table 2. It should be noted that both groups demonstrated progression of histomorphological changes from Day 3 to Day 10 of the experiment (Graph 1, Graph 2). More pronounced alterations were observed in animals with moderate and severe EAU. Beginning on Day 14, a reduction in inflammatory activity was observed, as reflected by the corresponding scores. However, by the end of the experiment, complete resolution of histomorphological changes was not observed in any of the animals (Graphs 1 and 2). Statistically significant differences between the groups were observed at all time points.

Table 1. Scale of pathomorphological changes in ocular structures in EAU

Morphological changes	Degree of inflammatory severity (score)		
	1	2	3
Cornea			
Endothelial infiltration	mild, perilimbal	moderate	intense, diffuse
Edema	mild	moderate	severe
Conjunctiva			
Infiltration (lymphocytes)	mild	moderate	intense, diffuse
Anterior chamber			
Flare	mild	moderate	severe
Inflammatory cell reaction	<5 cells/HPF	5–20 cells/HPF	20–50 cells/HPF, hypopyon
Iris			
Infiltration	mild, focal (lymphocytic)	moderate, multifocal (lymphocytic)	intense, diffuse (plasma cells, mast cells)
Synechiae	absent	isolated	multiple, complete posterior synechiae
Edema	mild	moderate	severe
Posterior chamber			
Exudate and infiltration	mild	moderate	severe
Ciliary body			
Infiltration	mild	moderate	severe
Edema	mild	moderate	severe
Vitreous body			
Infiltration	mild	moderate	intense, diffuse
Retina			
Exudative retinal detachment	mild, localized	moderate	total
Retinal inflammatory infiltration	mild	moderate	severe
Retinal pigment epithelium degeneration	mild	moderate	severe
Choroid			
Inflammatory infiltration	mild, focal	moderate, multifocal	severe, diffuse
Choroidal edema	mild	moderate	severe, with detachment

Cells/HPF – Cells per high-power field, EAU – experimental autoimmune uveitis

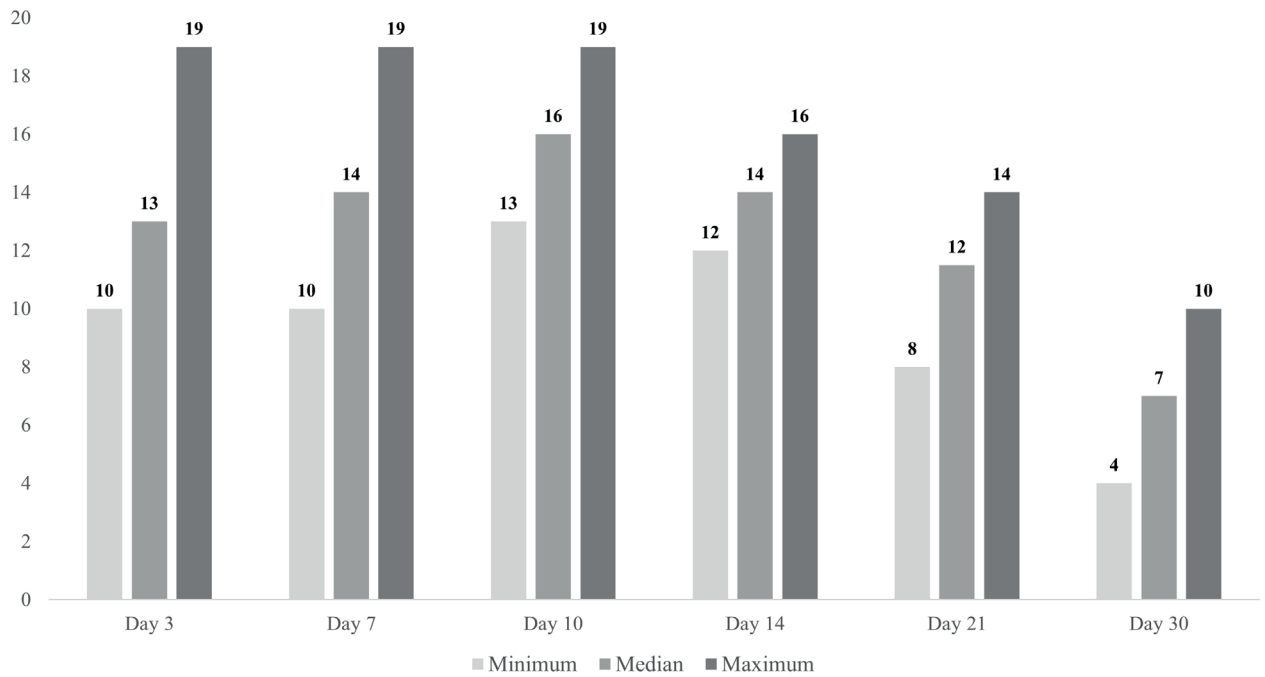

Graph 1. Dynamics of changes in the scoring values in Group I.

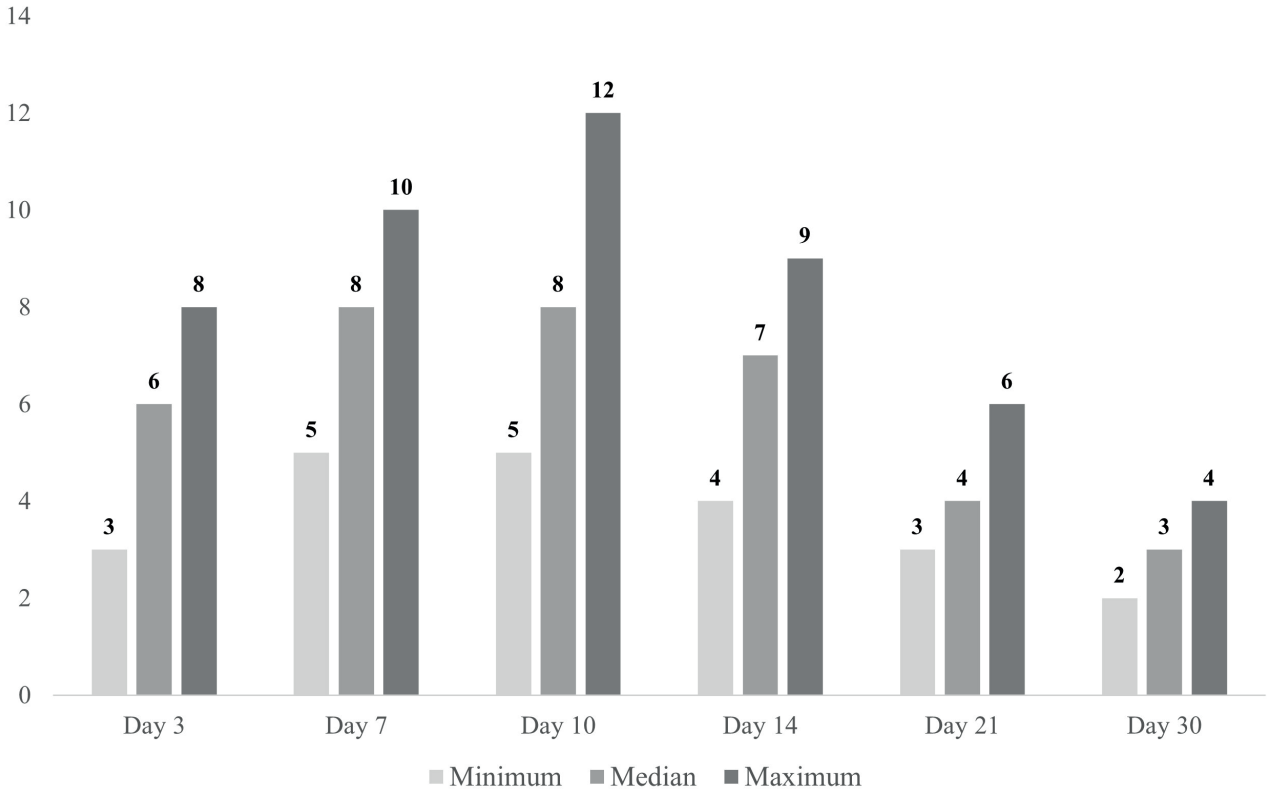

Graph 2. Dynamics of changes in the scoring values in Group II.

DISCUSSION

The histomorphological evaluation of uveitis is essential for understanding the pathogenesis, clinical course, and prognosis of the disease. Using this experimental model, we were able to demonstrate the spread of the inflammatory process within both the anterior and posterior segments of the eye at the morphological level. A number of published studies have described the clinical manifestations of intraocular inflammation [15,16], and the immunological alterations that occur in EAU [14,15,17]. However, clinical manifestations do not always reflect the full extent of intraocular damage. Histomorphological evaluation serves as an essential complement, providing detailed insight into the true severity and distribution of tissue injury. Although the literature includes descriptions of severe anterior segment involvement – occasionally even leading to corneal perforation – in experimental settings, such findings are not universal and depend on the specific model and immune response elicited [18]. However, several experimental models of autoimmune uveitis have been described, in which the inflammatory process predominantly affects the posterior segment, involving the choroid and retina, while changes in the anterior segment remain minimal. These models underscore the variability of immune-mediated ocular injury and highlight the importance of histological assessment in accurately characterizing the pattern and severity of inflammation. [19,21,22,29]. In our model of autoimmune uveitis, we observed a comparable morphological pattern.

Histomorphological evaluation in autoimmune uveitis is crucial for differentiating the type of inflammation (granulomatous vs non-granulomatous), elucidating the underlying pathogenic mechanisms (cell-mediated versus humoral), characterizing the cellular composition of the infiltrate, and identifying the presence of necrosis, vasculitis of the choroidal and retinal vessels, or destruction of the retinal pigment epithelium. In our study, we observed a humoral-type hypersensitivity reaction, predominantly involving lymphohistiocytic cells. The inflammatory infiltrate contained plasma cell-type elements and tissue basophils (mast cells).

Histological assessment also enabled evaluation of the structural alterations within the retina. Specifically, damage to the retinal pigment epithelium was identified, most pronounced in the optical portion of the retina. Choroidal vascular involvement was manifested as marked vascular dilation, accompanied by exudative stromal changes within the uveal tract. Retinal alterations were characterized primarily by injury to the inner retinal layers, attributable to vascular involvement and accompanied by a robust inflammatory response within the vitreous body. Notably, the photoreceptor layer remained preserved in most cases. In contrast, destruction of the retinal pigment epithelium was linked to damage of Bruch's membrane.

The literature provides no comparative description of morphological changes in autoimmune uveitis across different degrees of disease severity, which we were able to perform in the present study. The comparative analysis between experimental groups revealed marked differences. In Group I, where undiluted normal horse serum was injected intravitreally, the inflammatory response was significantly more pronounced. These eyes exhibited diffuse choroidal and retinal infiltration, extensive disruption of the retinal layers, involvement of the vitreous body, and destructive changes within the RPE. Exudative retinal detachment, widespread infiltration along the RPE–choroid interface, and occasional inflammatory foci within the optic nerve sheaths reflected the high severity of the induced immune reaction.

In contrast, Group II displayed a more heterogeneous spectrum of changes. While some eyes demonstrated only mild anterior segment involvement with intact retina and choroid, others developed moderate uveitic alterations, characterized by localized lymphocytic infiltrates in the ciliary body and zonular fibers, small focal choroidal infiltrates near the ora serrata, and limited preretinal cellular aggregates. Importantly, even in these cases, the structural integrity of most retinal layers remained preserved, indicating a substantially lower level of immune-mediated tissue injury, compared with Group I.

Overall, the findings confirm that the model effectively reproduces key morphological features of autoimmune uveitis, including posterior-predominant inflammation, vascular-mediated retinal injury, and secondary disturbances of the retinal pigment epithelium – Bruch's membrane complex. The distinct severity patterns observed between the experimental groups highlight the dose- and compartment-dependent nature of the immune response, as well as the importance of antigen accessibility within the uveal tract. These results contribute to a better understanding of the pathophysiological mechanisms underlying immune-mediated intraocular inflammation and provide a basis for future studies aimed at evaluating therapeutic interventions and identifying early structural biomarkers of disease activity.

CONCLUSION

In conclusion, histomorphological alterations in EAU demonstrated a clear time-dependent progression, reaching peak severity between Days 3 and 10, particularly in cases of moderate and severe disease. Although a partial reduction in inflammatory activity was observed from Day 14 onward, complete morphological recovery was not achieved by the end of the experimental period. The persistence of statistically significant differences between groups at all time points underscores the sustained impact of disease severity on ocular tissue damage and highlights the chronic and incompletely reversible nature of the inflammatory process in EAU.

Thus, the study of histomorphological changes in the eye during EAU allows for the assessment of the extent and severity of tissue damage, as well as the early detection of potential complications such as choroidal atrophy, glaucoma, and retinal degeneration, even before their clinical manifestations appear. In addition, it enables evaluation of the tissue's regenerative potential, which can inform therapeutic decision-making and provide a basis for assessing the efficacy of novel treatment approaches in the future.

REFERENCES

1. Biswas J, Annamalai R, Krishnaraj V. Biopsy pathology in uveitis. Middle East Afr J Ophthalmol. 2011;18(3):232-238.
2. Hysa E, Cutolo CA, Gotelli E, et al. Immunopathophysiology and clinical impact of uveitis in inflammatory rheumatic diseases: an update. Eur J Clin Invest. 2021;51(12):e13572.
3. London NJS, Rathinam SR, Cunningham ETJr. The epidemiology of uveitis in developing countries. Int Ophthalmol Clin. 2010;50(2):1-17.
4. Tomkins-Netzer O, Talat L, Bar A, et al. Long-term clinical outcome and causes of vision loss in patients with uveitis. Ophthalmology. 2014;121(12):2387-2392.
5. Durrani OM, Tehrani NN, Marr J.E, Moradi P, Stavrou P, Murray P.I. Degree, duration, and causes of visual loss in uveitis.Br J Ophthalmol. 2004;88(9):1159-1162.
6. Bansal S, Barathi VA, Iwata D, Agrawal R. Experimental autoimmune uveitis and other animal models of uveitis: An update. Indian J Ophthalmol. 2015;63(3):211–218.
7. Bora NS, Sohn JH, Kang SG, et al. Type I collagen is the autoantigen in experimental autoimmune anterior uveitis. J Immunol. 2004;172:7086-7094.
8. Horai R, Silver PB, Agarwal RK, et al. Breakdown of immune privilege and spontaneous autoimmunity in mice expressing a retina-specific T cell receptor. Int Immunol. 2010;22:21.
9. Zernii EY, Baksheeva VE, Iomdina EN, et al. Rabbit Models of Ocular Diseases: New Relevance for Classical Approaches. CNS Neurol Disord Drug Targets. 2016;15(3):267-91.
10. Brown SDM. Advances in mouse genetics for the study of human disease. Human Molecular Genetics. 2021;30(2):274-284.
11. Babinet C. Transgenic mice: an irreplaceable tool for the study of mammalian development and biology. J Am Soc Nephrol. 2000;16:88-94.
12. Pasechnikova NV, Zborovska OV, Nasinnyk IO, Velichko LM, Bohdanova OV, inventors; SI "The Filatov Institute of Eye Diseases and Tissue Therapy of NAMS of Ukraine". Method of simultaneous modeling of autoimmune uveitis of various severity levels. Ukraine patent UA 112120. 2016 Dec 12.
13. Smalyuh NV. Experimental justification of phonophoresis of fluorafur and its application in the treatment of endogenous uveitis [author's abstract for the dissertation] Odessa; 1986.
14. Kuryltsiv N, Zborovska O, Velychko L, Bohdanova A. T-Cells Response in Experimental Autoimmune Uveitis of Varying Severity. Ceska a slovenska oftalmologie. 2024;80:1-8.
15. Fan N-W, Li Y, Mittal SK, et al. Characterization of Clinical and Immune Responses in an Experimental Chronic Autoimmune Uveitis Model. Am J Pathol. 2021 Mar;191(3):425-437.
16. Kuryltsiv NB, Zborovska OV, Velychko LM, Khyrivskyi AL. Dynamics of theinflammatory biomarker neopterin level in experimental non-infectious autoimmune uveitis. Lviv Clinical Bulletin. 2022;3(39) - 4(40):33-39.
17. Caspi RR. Understanding Autoimmune Uveitis through Animal Models. Invest Ophthalmol Vis Sci. 2011 Mar;52(3):1873-1879.

18. Agarwal A, Agarwal RK, Silver PB, Caspi RR. Rodent models of experimental autoimmune uveitis. Int J Inflam. 2012;2012:1-18.
19. McMenamin PG, Broekhuyse RM, Forrester JV. Ultrastructural pathology of experimental autoimmune uveitis: A review. Micron. 1993; 24(5):521-546.
20. Dua HS. Ultrastructural pathology of experimental autoimmune uveitis. Eye (Lond). 1993;7:567-575.
21. Côté MA, Rao NA. The role of histopathology in the diagnosis and management of intraocular inflammatory disease. Can J Ophthalmol. 1990;25(6):283-289.
22. Lim LL, Suhler EB, Rosenbaum JT, Wilson DJ. The role of choroidal and retinal biopsies in the diagnosis and management of atypical presentations of uveitis. Trans Am Ophthalmol Soc. 2005;103:84-91.